TISSUE ENGINEERING: Part C
Volume 22, Number 9, 2016
© Mary Ann Liebert, Inc.
DOI: 10.1089/ten.tec.2016.0053

termis
Tissue Engineering
& Regenerative Medicine
International Society

METHODS ARTICLE

A Flow Perfusion Bioreactor System for Vocal Fold Tissue Engineering Applications

Neda Latifi, MSc,[1] Hossein K. Heris, PhD,[1] Scott L. Thomson, PhD,[2] Rani Taher, PhD,[1,*] Siavash Kazemirad, PhD,[1] Sara Sheibani, PhD,[3,†] Nicole Y.K. Li-Jessen, PhD,[4] Hojatollah Vali, PhD,[3] and Luc Mongeau, PhD[1]

The human vocal folds (VFs) undergo complex biomechanical stimulation during phonation. The aim of the present study was to develop and validate a phono-mimetic VF flow perfusion bioreactor, which mimics the mechanical microenvironment of the human VFs *in vitro*. The bioreactor uses airflow-induced self-oscillations, which have been shown to produce mechanical loading and contact forces that are representative of human phonation. The bioreactor consisted of two synthetic VF replicas within a silicone body. A cell-scaffold mixture (CSM) consisting of human VF fibroblasts, hyaluronic acid, gelatin, and a polyethylene glycol cross-linker was injected into cavities within the replicas. Cell culture medium (CCM) was perfused through the scaffold by using a customized secondary flow loop. After the injection, the bioreactor was operated with no stimulation over a 3-day period to allow for cell adaptation. Phonation was subsequently induced by using a variable speed centrifugal blower for 2 h each day over a period of 4 days. A similar bioreactor without biomechanical stimulation was used as the nonphonatory control. The CSM was harvested from both VF replicas 7 days after the injection. The results confirmed that the phono-mimetic bioreactor supports cell viability and extracellular matrix proteins synthesis, as expected. Many scaffold materials were found to degrade because of challenges from phonation-induced biomechanical stimulation as well as due to biochemical reactions with the CCM. The bioreactor concept enables future investigations of the effects of different phonatory characteristics, that is, voice regimes, on the behavior of the human VF cells. It will also help study the long-term functional outcomes of the VF-specific biomaterials before animal and clinical studies.

Introduction

The human vocal folds (VFs) include the lamina propria (LP), very soft tissue located on opposite sides of the larynx. Human phonation involves a transfer of energy between air expelled by the lungs and airflow-induced self-sustained oscillations of the VFs, accompanied by pulsatile airflow through the airway (Fig. 1A). During phonation, the VFs oscillate at fundamental frequencies between 100 and 200 cycles per second, causing periodic opening and closing of the glottis (Fig. 1B, C). This is usually accompanied by collision between the folds. Sound waves produced by the unsteady glottal mass flow drive high-amplitude acoustic standing waves within the vocal tract, along with traveling waves propagating along the inferior direction toward the bronchi. The LP, therefore, experiences complex high-frequency biomechanical stimulation during phonation, involving tensile, contractile, aerodynamic, impact, and shear stresses.[1]

The most severe disorders affecting voice are those in which a part of the soft LP is either lost or replaced by stiff fibrous tissue. In ideal cases, injectable biomaterials are used to regenerate the extracellular matrix (ECM) in the LP and to restore the viscoelastic functions of the damaged VF tissue.[2–4] One challenge in designing VF-specific biomaterials is that their long-term functional outcomes are complicated by the phonation-induced biomechanical stimulation. In addition to the cell-biomaterial interactions that are pertinent to the chemical properties of the biomaterials, biomechanical stimulation also affects cell functions in VF growth and regeneration.[1,5] Previous studies have shown that human VF LP evolves from a homogenous one-layer

[1]Department of Mechanical Engineering, McGill University, Montreal, Canada.
[2]Department of Mechanical Engineering, Brigham Young University, Provo, Utah.
[3]Department of Anatomy and Cell Biology, McGill University, Montreal, Canada.
[4]School of Communication Sciences and Disorders, McGill University, Montreal, Canada.
Current affiliation: American University of the Middle East, Eqaila, Kuwait.
†Current affiliation: Defence Research and Development Canada, Medicine Hat, Canada.

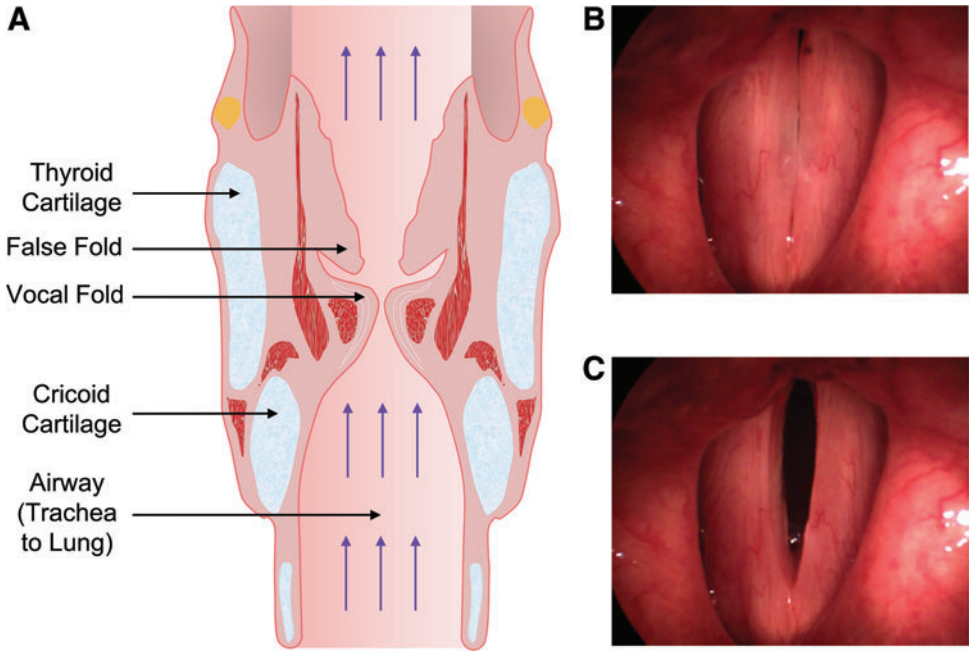

FIG. 1. Anatomy of the human larynx. **(A)** Coronal section of the larynx. The picture was reproduced from https://classconnection.s3.amazonaws.com/158/flashcards/2547158/jpg/sphincters_of_larynx1361134532658.jpg **(B)** and **(C)** pictures of two vocal folds during phonation. Vocal folds are stretched longitudinally and oscillate laterally perpendicular to their longitudinal axis. The glottis, that is, the gap between the vocal folds, repeatedly opens and closes during phonation. Color images available online at www.liebertpub.com/tec

structure in newborn infants to a three-layer structure over the period between the age of 7 and 12 years old,[6] and the final multi-layer organization of collagen and elastin fibers is formed around the age of 13.[7] Investigations of unphonated human patients have suggested that biomechanical stimulation is one of the factors in the development of the LP microstructure.[6,8] A good understanding of the effects of phonation-induced biomechanical stimulation on ECM growth and remodeling is, thus, required to engineer VF-specific biomaterials.[1]

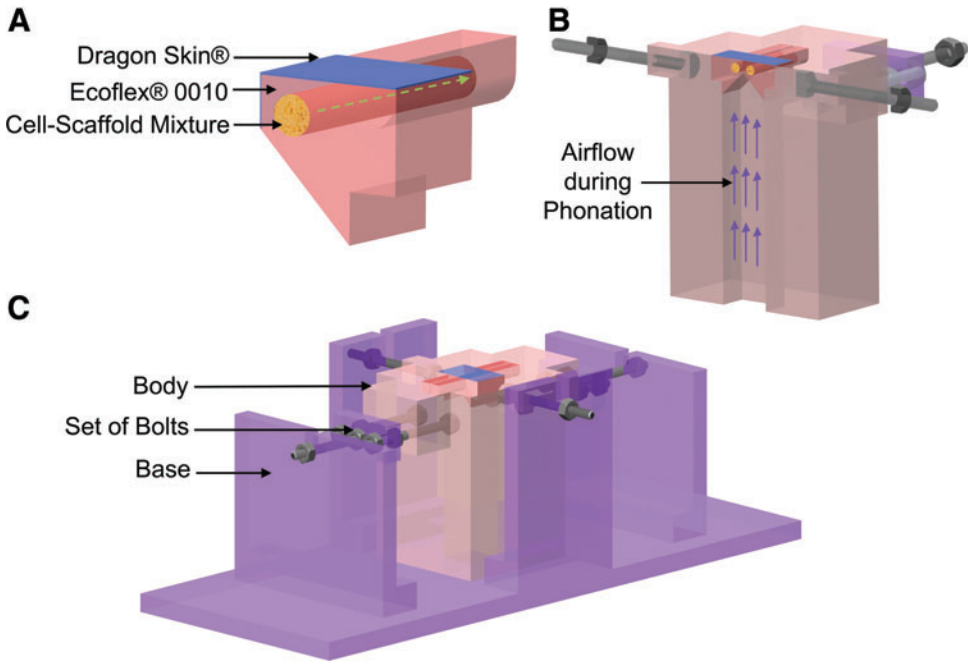

FIG. 2. Computer-aided design drawings of the bioreactor. **(A)** A 3D section of the synthetic vocal fold replica at the center and perpendicular to the longitudinal axis. The replica has a layered structure. The innermost layer consists of the CSM, which was injected inside a cylindrical inner cavity. The main layer was fabricated by using Ecoflex® 0010. An ~100-μm-thick layer of Dragon Skin®, shown in *blue*, was added to the vibrating portion of the replica to decrease tackiness, increase model durability, and improve phonatory characteristics. The flow of CCM through the CSM is shown by using the *green dashed arrow*. **(B)** A 3D section of the bioreactor body. The lateral position of the two vocal fold replicas is shown in the section view. The direction of airflow during phonation is shown by using the *purple arrows*. **(C)** The bioreactor body is installed on a Plexiglas base before the CSM injection. 3D, three-dimensional; CCM, cell culture medium; CSM, cell-scaffold mixture. Color images available online at www.liebertpub.com/tec

To this end, a controlled experimental environment is useful to reproduce the phonation-induced biomechanical stimulation *in vitro*, and to systematically investigate its influence on the behavior of VF cells that are encapsulated within the biomaterial. A bioreactor offers a biomimetic culture environment that allows the effects of biochemical and biomechanical factors to be evaluated systematically, in particular for cells that are encapsulated in biomaterial products for VF tissue engineering. Bioreactors are also useful as mimetic platforms to investigate the mechanical stability of the biomaterials under realistic stimulation. This approach allows the characterization of potential scaffold biomaterials *in vitro* at a lower cost before animal and clinical studies.

Efforts have been made to build such VF bioreactors over the past 15 years, as summarized in Table 1.[9–15] The first mechanically driven VF bioreactor was designed to impose a 20% static axial strain and a 100 Hz vibratory stimulation for 6 h on human laryngeal fibroblasts seeded in three-dimensional (3D) Tecoflex® porous substrates.[9] A modest increase in the cell density was observed along with slightly greater amounts of major ECM proteins in the stimulated samples than in the controls. Another mechanically driven bioreactor was developed to investigate the effects of high-frequency substrate vibratory stimulation at 100 Hz on human laryngeal fibroblasts seeded in 3D Tecoflex substrates.[10] The cells were stimulated for 14 min per day over 21 days. A significant increase in collagen type I (Col-I) densities was observed relative to the controls, but mostly over the surface of the Tecoflex substrate. Cell viability was not examined. In another mechanically driven bioreactor study, the effects of high-frequency vibrations on the activity and ECM synthesis of human dermal fibroblasts were investigated.[11] The results indicated a relatively low cell viability rate and a corresponding decrease in Col-I synthesis relative to the static controls. In a separate study, the influence of cyclic equibiaxial tensile strain on rabbit VF fibroblasts was investigated.[12] The cell monolayer was cultured on Col-I-coated Bioflex® II plates, and it was stimulated for 4 h per day over a duration of 1/2 days. This bioreactor supported cell viability. No protein analysis at the ECM level was performed, and the stimulation frequency range was limited to $0.005 - 0.5$ Hz, which is much lower than the human phonation range. In another mechanically driven bioreactor, Titze *et al.*'s bioreactor concept[9] was revisited to incorporate a mechanism for VF collision.[13] The influence of vibratory stimulation, 20% axial strain, and VF collision on human VF fibroblasts and human bone marrow mesenchymal stem cells was investigated. The cells were stimulated for 8 h over a duration of 1 day. No myofibroblast differentiation occurred for either cell lines.

It has been acknowledged that substrate vibratory stimulation and/or cyclic tensile straining may not constitute a realistic biomechanical stimulation.[14] Aerodynamic stresses associated with the glottal wall pressure field, compression and impact stresses related to VF collision, and shear stresses involved in the propagation of a mucosal wave are also believed to contribute to the overall stress and strain fields during phonation. This observation has spurred the creation of bioreactors that are better tailored to phonation. An electro-acoustically driven bioreactor was developed toward that end.[14] This bioreactor used a loudspeaker to stimulate the cell monolayer cultured on a Col-I-coated silicone membrane by using acoustic waves. The cells were stimulated for an hour over a duration of 1 day. A more realistic cell response in terms of gene expression of Col-I and hyaluronic acid (HA) was observed than in the mechanically driven VF bioreactors. The concept of this bioreactor was then revisited to stimulate human bone marrow mesenchymal stem cells that were cultured in a 3D fibrous scaffold with physiologically relevant high-frequency vibration.[5,15] Cells were shown to be actively involved in producing ECM proteins. No significant alterations in the collagen synthesis were observed between the stimulated samples and the static controls. The acoustic stimulation used in these bioreactors, however, mimicked neither VF collisions nor the aerodynamic pressure involved in phonation.

The goal of the present study was to create and evaluate a novel VF bioreactor concept. A flow perfusion design was selected to feed the cells with appropriate concentrations of gases and nutrients. Mass transport is one of the most critical biological factors for various cell behaviors.[16] Flow perfusion bioreactors have been previously developed for bone, heart, and cartilage tissue engineering.[17,18] The perfusion facilitates the transport of nutrients to cells and the removal of toxic metabolites through interconnected scaffold pores, thus promoting cellular viability, proliferation, and differentiation.[18] In confined perfusion bioreactors, the cell-scaffold mixture (CSM) is confined within an individual chamber to force the cell culture medium (CCM) to perfuse through its pores.[18] Enhanced cell differentiation and more uniform cell distribution have been achieved in such bioreactors than in unconfined perfusion bioreactors.[19]

In the present study, the concept of confined perfusion was adapted through the inclusion of a perfusion loop in a new bioreactor concept composed of two synthetic VF replicas located within a silicone body to achieve a better reproduction of the physiological phonation environment *in vitro*.[20,21] The perfusion loop ensures nutrient mass transport; whereas the cells are stimulated with the targeted phonation-induced mechanical loads via the airflow-induced self-oscillations of the VF replicas, which have demonstrated vibratory characteristics similar to those of human VFs.[22] This bioreactor mimics the airflow-induced biomechanical stimulation involved in human phonation, including the collisions between the folds and the wall pressure changes associated with airflow. Various HA–gelatin scaffolds were seeded with human vocal fold fibroblasts (HVFFs). Preliminary cell viability and collagen analysis were performed to examine whether or not the novel bioreactor supports *in vitro* cell culture.

Materials and Methods

Bioreactor design

The bioreactor consists of a pair of VF replicas (Fig. 2A), mounted on a custom-built body (Fig. 2B) connected to an air blower, a pressure transducer, and a sound level meter, which are housed in a tissue culture incubator (CO_2 Incubator NU AIRE Model NU-5510; NuAire, Inc., Plymouth, MN). See Supplementary Figure S1 (Supplementary Data are available online at www.liebertpub.com/tec) for the actual bioreactor setup inside the incubator. The commercial incubator was used to maintain a temperature of 37°C and a relative humidity of around 95%. The VF replicas were made of two layers of silicone rubber, namely, Dragon

Table 1. Summary Table for the Vocal Fold Bioreactors Cited Within the Article

References	*Titze et al.*[9]	*Wolchok et al.*[10]	*Kutty and Webb*[11]	*Branski et al.*[12]	*Gaston et al.*[13]	*Farran et al.*[14]	*Tong et al.*[15]	*Present study*
Reactor type	3D-axial and vibratory stimulation	3D-substrate vibratory stimulation	3D-vibratory stimulation	2D-cyclic equibiaxial tensile strain	3D-axial and vibratory stimulation	2D-electro-acoustically driven	3D-electro-acoustically driven	3D-perfusion phonation-induced stimulation
Cell line	Human laryngeal fibroblasts	Human laryngeal fibroblasts	Human dermal fibroblasts	Rabbit vocal fold fibroblasts	Human vocal fold fibroblasts or human bone marrow MSCs	Human neonatal foreskin fibroblasts	Human bone marrow MSCs	Human vocal fold fibroblasts
Culture substrate or scaffold type	Tecoflex® substrate	Tecoflex substrate	Methacrylated hyaluronate hydrogel	Cell monolayer on collagen type I-coated Bioflex® II	Fibronectin-coated Tecoflex substrate	Cell monolayer on collagen type I-coated silicone membrane	Fibrous PCL scaffold	HA–Ge hydrogel
CCM composition	DMEM/F12 and 10% FBS[1]	DMEM/F12, 10% FBS, and 176.12 μg/mL ascorbic acid	DMEM/F12 and 10% FBS[2]	DMEM without FBS[3]	DMEM or α-MEM and 10% FBS[4]	Fibroblast basal medium and fibroblast low-serum growth kit[5]	MSC maintenance medium	DMEM, 5% FBS and 50 μg/mL ascorbic acid[6]
Stimulation frequency (Hz)	100	100	100	0.005–0.5	200	0–400	200	~100
Static culture before stimulation (days)	3	2	Overnight	4–5	Not reported	1	3	3
Tensile stresses	✓	×	×	✓	✓	✓	✓	✓
Compressive stresses	×	×	×	×	×	✓	✓	✓
Aerodynamic stresses	×	×	×	×	×	×	×	✓
Impact stresses	×	×	×	×	✓	×	×	✓
Phonation-induced stimulation	×	×	×	×	×	×	×	✓
Mucosal wave propagation	×	×	×	×	×	×	×	✓
Longitudinal prestretch (%)	20	×	×	×	20	×	×	10
Scaffold shape	Cubic	Cubic	Not reported	N/A	Cubic	N/A	A narrow groove in a silicone disk	Cylindrical[7]
Stimulation duration per day	6 h	14 min	4 h	4 h	8 h	1 h	12 h	2 h
Duration (days)	1, 7	21	10	1 or 2	1	1	7	4
Cell viability	>95%, Not reported	Not examined	<60%	>99%	>96%	Not examined	Qualitatively similar to the static controls	>90%
Collagen type I synthesis (ECM level)	✓ (Little accumulation)	✓ (Mostly at the surface)	✓ (Lower than the static controls)	×	×	×	✓ (No significant alterations)	✓ (Significantly greater than the controls)
Collagen type III synthesis (ECM level)	×	×	×	×	×	×	✓ (No significant alterations)	✓ (Significantly greater than the controls)

[1]The medium also contained 25 μg/mL gentamicin.
[2]The medium also contained 1 × L-glutamine, 15 mM HEPES, 50 U/mL penicillin, and 50 μg/mL streptomycin.
[3]Four different medium compositions were investigated.[12]
[4]The medium also contained 1% penicillin/streptomycin, and 1% nonessential amino acids. For the stem cells, the medium contained 1% L-glutamine as well.
[5]The medium also contained 1% penicillin–streptomycin.
[6]Our medium also contained 1% penicillin/streptomycin, 1% sodium pyruvate, and 1% MEM nonessential amino acids.
[7]The cell-scaffold mixture was placed in a cylindrical cavity that was ~4 mm in diameter and 50 mm in length (Refer to Bioreactor Design section for detailed information).

2D, two-dimensional culture; 3D, three-dimensional; CCM, cell culture medium; DMEM, Dulbecco's modified Eagle medium; ECM, extracellular matrix; FBS, fetal bovine serum; Ge, gelatin; HA, hyaluronic acid; MEM, minimum essential medium; MSCs, mesenchymal stem cells.

Skin® and Ecoflex® 0010 Platinum Cure Silicone Rubber (Smooth-On, Easton, PA), surrounding a cylindrical cavity ($\sim$4 mm in diameter and 50 mm in length) hosting the CSM (Fig. 2A). The geometry of the vibrating portion of the VF replicas was similar to that of the *M5* rigid model.[23] The two replicas were placed in lateral contact, resembling the collision contact between the two human VFs in the larynx (Figs. 1 and 2B). To mimic longitudinally stretching of the human VFs during phonation (Fig. 1B), two sets of bolts were used to adjust the longitudinal prestretch of the replicas (Fig. 2C). The bioreactor body was mounted on a Plexiglas base before loading the CSM (Fig. 2C). The base was connected to a variable speed centrifugal air blower that delivered the airflow needed for phonation (Supplementary Fig. S1). The airflow direction is shown by using the purple arrows in Figures 2B and 3.

A mixture of the CCM, oxygen, and carbon dioxide (CO_2) is perfused through the pores within the CSM along the longitudinal axis of each replica, as shown by using a green dashed arrow in Figure 2A. The perfusion flow rate was 0.01 mL/min.

Bioreactor fabrication

A 3D computer-aided design model of the VF replica mold was created by using SolidWorks 2011 (Dassault Systems SolidWorks Corp., Waltham, MA). The mold was fabricated by using a commercial 3D printer (Connex 500 multi-material 3D printer; Stratasys for a 3D World, Inc., Eden Prairie, MN). A cylindrical glass insert with an outer diameter of 4 mm was placed in the mold before the addition of the silicone rubber solution to create an inner cavity to host the CSM. The replica was fabricated by using a three-component addition-cure silicone, that is, two-part Ecoflex 0010 and single-part silicone thinner. Ingredients from the commercial package, that is, part A, part B, and silicone thinner, were mixed with a mass ratio of 1:1:1.5, respectively. The silicone thinner was added to achieve viscoelastic properties similar to those reported for cadaveric human VF cover, that is, a Young's modulus of around 3.0 kPa.[24] A vacuum pump was used to evacuate the mixture and to remove air bubbles. The mixture was subsequently molded and cured at room temperature for $\sim$6 h. The cured replica was removed from the mold, and unnecessary parts were trimmed. It was washed under the laminar hood with ethyl alcohol (70%), followed by deionized water. The inner cavity was cleaned to remove the residue of the release agent, which had been applied to facilitate release of the replica from the mold. After drying, additional Ecoflex solution was prepared and applied to close the open side of the replica (performed under the laminar hood). It was fully cured and unnecessary parts were trimmed.

An $\sim$100-μm-thick layer of Dragon Skin was applied on the superior surface of the vibrating portion of the replicas (Fig. 2A), to decrease tackiness, improve their phonatory characteristics,[25] and increase model durability. The latter was important given the low modulus of elasticity of the underlying Ecoflex 0010. The lateral side of the replica was placed on a flat surface with the medial surface facing up. Dragon Skin part A, part B, and silicone thinner were mixed with a mass ratio of 1:1:1. After removing air bubbles, the mixture was slowly poured over the replica. The process was repeated after 1 h to create a thicker layer. The excess material was removed with a razor blade.[25,26]

Three-dimensional sections of computer-aided design drawings of the replica and the bioreactor body are shown in Figure 2A and B, respectively. Ecoflex 0030 Platinum Cure Silicone Rubber (Smooth-On) was used to fabricate the body. The mold parts were cleaned with ethyl alcohol (70%), and a release agent was applied before casting. The parts were assembled, and two bolts were placed on each side of the longitudinal axis of the mold before the preparation of the silicone solution. An Ecoflex 0030 mixture was prepared with a mixing ratio of 1:1 for the silicone ingredients, that is, part A and part B. As for the replicas, the solution was placed in the vacuum chamber to remove air bubbles after mixing. The VF replicas were placed on a Plexiglas plate and aligned with contact. A thin plastic sheet was placed between them to reduce tackiness. The replicas were then positioned securely over the mold. Attention was paid to achieve a perfect contact between the replicas and the mold to prevent the silicone rubber solution from leaking into the gap. The solution was slowly poured into the mold to prevent the creation of new air bubbles. The body was cured at room temperature for 12 h. The entire body was carefully released from the mold and then autoclaved to sterilize the inner cavity of the replicas. Two rectangular Plexiglas plates attached to the bolts on each side of the body were used to impose a symmetric and approximately uniform longitudinal prestretch to both VF replicas (Fig. 2C).

Mechanical longevity test

Synthetic replicas such as those used in the present study have been shown to vibrate for extended periods without any significant changes in behavior. In the process of exploring the feasibility of using the synthetic replicas in the present bioreactor, one replica concept prototype, without interior cavity, was mounted on a flow supply setup and self-oscillated over 100 h (not continuously).

Cell culture in flask

Human VF fibroblasts were provided courtesy of Professor Susan Thibeault (Department of Surgery, University of Wisconsin-Madison). Cells were cultured in a mixture of Dulbecco's modified Eagle medium (DMEM; Life Technologies, Inc., Burlington, ON), 10% fetal bovine serum (FBS; Sigma-Aldrich Co., St. Louis, MO), 1% penicillin/streptomycin (P/S; Sigma-Aldrich Co.), 1% sodium pyruvate (Life Technologies, Inc.), and 1% minimum essential medium (MEM) nonessential amino acids (MNEAA; Sigma-Aldrich Co.) at 37°C, in a 5% CO_2 humidified atmosphere. All concentrations for the CCM ingredients are expressed as %v/v (volume-to-volume percentage). The CCM was replaced every 3 days. Cells were disassociated by using 0.25% trypsin-EDTA when they reached around 70% confluency. The cells were subsequently centrifuged and suspended with serum-free CCM.

CSM preparation and injection

Thiol-modified heparin-bonded HA and thiol-modified gelatin (Ge) were purchased from ESI BIO (BioTime, Inc., Alameda, CA). Polyethylene glycol (PEG) acrylate cross-

linkers (PEG di-acrylate [PEGDA] and PEG tetra-acrylate [PEGTA]) were provided by Laysan Bio, Inc. (Arab, AL). Solutions of 2.0% HA, 0.4% Ge, and 2.0% PEGTA cross-linker were prepared under the laminar hood to prevent contamination. All concentrations for the scaffold ingredients are expressed as %w/v (weight-to-volume percentage). The HA and Ge solutions were sonicated separately for 1 min. The CSM was prepared by using equal volume fractions of HVFFs solution (8×10^6 cells/mL), 2.0% HA, 0.4% Ge, and 2.0% PEGTA cross-linker.

The CSM was slowly injected into the replica cavity within 5–10 min of CSM preparation, before the hydrogel was fully cured, to ensure the integrity of the network and to prevent bubble creation. A second needle was inserted into the opposite side of each replica to release air from the cavity during the injection. The CCM (DMEM, 5% FBS, 1% P/S, 1% MNEAA, and 50 μg/mL ascorbic acid [Sigma-Aldrich Co.]) was mixed with a filtered mixture of 5% CO_2 and 95% air inside sterile intravenous bags, and it was connected to the replicas after the CSM injection. The replicas were kept inside the incubator for about 30 min before the introduction of the CCM perfusion flow, to ensure a cured cross-linked network. The CCM was perfused through the CSM at a rate of $\sim$0.01 mL/min. The perfusion rate was adjusted by using manual valves, and the rate was monitored every 60 min.

The control sample was prepared by following the same procedure. The CSM was encapsulated inside the cavity of one VF replica without being subjected to phonation. The CCM was perfused through the CSM with the same flow rate as for the bioreactor. The CSM was injected at the bottom of glass-bottom Petri dishes (MatTek, Inc., Ashland, MA) to monitor cell viability in the absence of flow perfusion and biomechanical stimulation. It was incubated under normal cell culture conditions in parallel with the bioreactor and control operation.

Mechanical stability (fatigue) test

Scaffolds were fabricated by using 0.50% HA, 0.25% Ge, and 0.50% PEGDA or 0.50% PEGTA, and they were injected into the cavities of one bioreactor. The bioreactor was then phonated continuously for 72 h. Subsequently, the scaffold was harvested and its mechanical integrity was evaluated visually. Some scaffolds exhibited evident fracture cracks after phonation, resulting in fragmentation. The examiner estimated the severity of fragmentation by counting the number of scaffold fragments. Scaffolds with 0.50% HA, 0.10% Ge, and 0.50% PEGDA or 0.50% PEGTA (see rationale in in the Discussion section) were examined by using the same procedure. The fatigue test was repeated three times for each scaffold composition.

Biochemical stability test

Five different concentrations of Ge (0.25%, 0.10%, 0.05%, 0.02%, and 0.00%) and two different PEG cross-linkers (0.50% PEGDA and 0.50% PEGTA) were used. CSMs with different concentrations of the constituents were submerged in CCM with different FBS concentrations (2%, 5%, and 10%) in static condition at 37°C. The medium was changed every day. Another set of samples was submerged in distilled water to study hydrolysis. The samples were inspected visually for their integrity at 3, 5, 7, 14, and 21 days after the injection.

Rheometry

A TA Instrument Rheometer-AR2000 (New Castle, DE) was used to measure the shear elastic and loss moduli of the silicone rubbers that were used in the fabrication of the replicas. Parallel plates with a diameter of 25 mm and a gap of 600 μm were used. The distance between the two plates was calibrated before the measurements. The shear moduli of the samples were measured within the frequency range between 0.5 and 100.0 Hz. A strain sweep test was also performed over a strain range of 1 – 1000% at the frequency of 1 Hz. The corresponding oscillatory stress–strain curves were obtained.

Similar procedures were followed to measure the viscoelastic properties of the HA–Ge hydrogels at room temperature. Parallel plates with a diameter of 25 mm and a gap of 200 μm were used. The sample was prepared in syringes and injected to completely fill the gap between the plates. After 15 min, water was injected into the surroundings of the sample to prevent dehydration. A controlled stress frequency sweep test was performed over the frequency range between 0.5 and 100.0 Hz, followed by a strain sweep step at the frequency of 1.0 Hz.

Phonatory stimulation

The bioreactor was loaded with the selected CSM, that is, the scaffold of 0.50% HA, 0.10% Ge, 0.50% PEGTA, and HVFFs solution (2×10^6 cells/mL) based on the mechanical and biochemical tests (see Mechanical stability test and Biochemical stability test sections). The bioreactor was first operated without phonatory stimulation for a duration of 3 days.[9,15,27,28] Subsequently, the bioreactor was phonated for 2 h each day over a period of 4 days. The bioreactor was phonated for 1 h, rested for 15 min, and phonated for another hour. The folds were unstretched while the bioreactor was not phonating. During phonation, the CCM flow was temporarily suspended, and a longitudinal prestretch of $\sim$10% was applied. A schematic of the phonation setup is shown in Figure 3. The variable speed centrifugal blower was connected to the base with a 20 cm-long tube. A high-resolution pressure transducer (PCB Piezotronics, Inc., Depew, NY) was mounted under the base, $\sim$10 cm below the folds, to measure the dynamic subglottal pressure. The transducer was connected to a power supply (PCB Piezotronics, Inc.), which, in turn, was connected to a data acquisition system (Data Translation, Inc., Marlboro, MA). The dynamic supraglottal pressure was monitored by using a digital sound level meter (RadioShack Corporation, Fort Worth, TX) about 10 cm away from the folds. The data from the sound level meter were obtained synchronously by using the same data acquisition system. A Baratron differential capacitance manometer (type 220; MKS Instruments, Inc., Andover, MA) was used to measure the static subglottal pressure 10 cm below the folds. The data were displayed by using an MKS PR 4000F digital readout. The CCM perfusion was resumed immediately after phonation. The bioreactor was visually inspected every day to verify the stability of the shape and size of the folds over time. Three bioreactors were operated by following the same procedure.

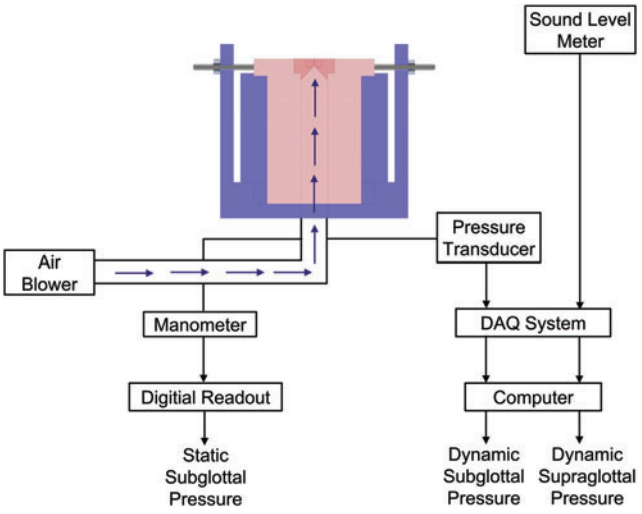

FIG. 3. Schematic of the bioreactor system during phonation. DAQ, data acquisition system. Color images available online at www.liebertpub.com/tec

Cell viability

The CSM was harvested after 7 days of culturing inside the bioreactor. The LIVE/DEAD® Viability/Cytotoxicity kit (Life Technologies, Inc.) was used to assess the viability of the cells in the central part of the phonated and un-phonated samples. The kit provides a two-color fluorescent image. Calcein-AM specifically stains live cells via intracellular esterase activity. Ethidium homodimer-1 (EthD-1) specifically stains dead cells that have lost plasma membrane integrity. The CSM samples were washed three times for 5 min each (3 × 5 min) by using 1× phosphate-buffered saline (PBS). The samples were then incubated with working solution (2 μM calcein-AM and 4 μM EthD-1 in Dulbecco's phosphate-buffered saline [DPBS; Life Technologies, Inc.]) for 30 min in darkness at room temperature. They were then washed again in 1× PBS for 3 × 5 min.

Extracellular matrix proteins staining

Immunohistochemistry was performed to stain Col-I, and Col-III of the zero time point (i.e., at the time of injection), control (with CCM flow and without phonation), and the phonated samples. The harvested CSM, containing cells, HA–Ge hydrogel, and synthesized ECM proteins, was embedded in 0.4% paraformaldehyde (Abcam, Inc.) in 1× PBS at 4°C overnight. The fixed CSM was washed in 1× PBS for 3 × 5 min. The sample was blocked by using goat serum (Abcam, Inc.) in 1× PBS (1:20) for 30 min. The blocked sample was washed by using 1× PBS for 3 × 5 min and incubated with the associated primary rabbit polyclonal antibody of Col-I (ab34710), or Col-III (ab59436) (Abcam, Inc.) for 1 h at room temperature. After washing the sample with 1× PBS for 3 × 10 min, the sample was blocked again by using goat serum in 1× PBS for 30 min. The sample was subsequently incubated for 1 h with the secondary antibody, Alexa Fluor® 488 goat anti-rabbit IgG (A-11034; Molecular Probes), at room temperature. The sample was washed again by using 1× PBS for 3 × 10 min. The stained samples were placed at the bottom of 35 mm glass-bottom Petri dishes (MatTek, Inc.). DAPI (4′,6-diamidino-2-phenylindole dihydrochloride) staining was performed at the time of microscopy to stain the cell nuclei in blue.

Confocal fluorescence microscopy and image analysis

An inverted confocal fluorescence microscope (LSM710; Zeiss, Jena, Germany) was used to image the stained samples. All the images were acquired by using a 20× objective (20 × /0.8 Dry Plan-Apochromat; Zeiss). A series of XY images, forming a Z-stack, were collected by using voxel sizes of 0.145, 0.145, and 10.000 μm along the *x*-, *y*-, and *z*-directions, respectively. The resolution of the acquired images was 1024 × 1024 pixels coded in 12 bits for each color channel. Image acquisition and image analysis, including 3D reconstruction, were performed using the software Zen (Zeiss) and Imaris version 7.5.6 (Bitplane, South Windsor, CT), respectively.

In Imaris, the surface function was used to create an isosurface of each stained object (cell nuclei or ECM proteins). A ''surface area detail level'' setting of 0.435 μm was used. Setting values for ''background subtraction with diameter of largest sphere which fits into the object'' of 0.830 and 0.300 μm were applied to detect the cell nuclei and the ECM proteins, respectively. For each group of images (i.e., viability, Col-I/DAPI, and Col-III/DAPI), the phonated samples were first analyzed. The surfaces of the stained objects were generated by using the intensity thresholding that was automatically determined by the software. The Imaris automatic thresholding is based on k-means clustering and dividing the image intensity histogram into two populations by using a previously verified algorithm.[29] This method of thresholding offers a robust way to identify the boundaries of the stained objects without any user bias.[30] When necessary, a minimum voxel threshold filter was

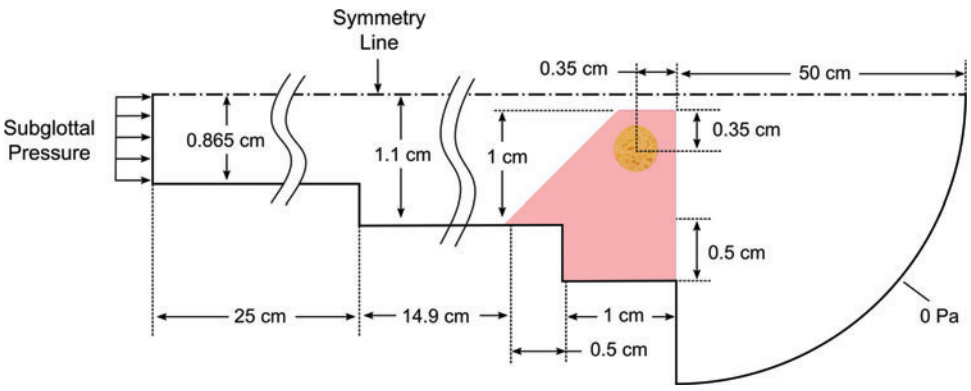

FIG. 4. Fluid and solid computational model domains (not to scale) (Refer to Fig. 2 for the layered structure of the vocal fold replica). Color images available online at www.liebertpub.com/tec

Table 2. Material Properties Used in the Computational Model

Region	*Replica constituents*	*Young's modulus (Pa)*	*Bulk modulus (kPa)*	*Density (kg/m^3)*
Outer layer	Dragon Skin®	31027.5	5171.25	1070
Main layer	Ecoflex® 0010	9693	1615.50	1040
Cell-scaffold mixture	HA–Ge–PEGTA	588.9	98.15	1000

The scaffold mixture with 0.50% HA, 0.1% Ge, and 0.50% PEGTA cross-linker was used for computational modeling.
HA, hyaluronic acid; PEGTA, polyethylene glycol tetra-acrylate.

applied on the selections to remove small-volume object artifacts. For other conditions (i.e., control and zero time point), the images were analyzed with the same settings as for the phonated sample.

The viability rate was calculated as the number of live cells divided by the total number of cells (i.e., the number of both live and dead cells) in each 3D image. The normalized number of cells was then obtained by dividing the number of cells (live, dead, or the total) by the volume of the image. The total volume of the detected ECM objects signal over the volume of the acquired image was calculated to obtain the signal density of the synthesized ECM proteins. Statistical significance was determined by a paired student's *t*-test, when applicable. Differences were considered significant at $p < 0.05$.

Computational model

Computational simulations were performed to estimate the time-dependent stress field within the replica cavity. The model was developed by using the commercial solver ADINA (ADINA R&D, Inc., Watertown, MA). It consisted of separate, but fully coupled, two-dimensional fluid and solid domains, as shown in Figure 4. The model was evolved from previously developed models, which have been verified and used to study VF vibrations.[31–34]

The fluid domain was governed by using the viscous, unsteady Navier–Stokes equations. The flow was assumed to be laminar and slightly compressible, with the latter allowing for acoustical effects to be modeled.[31] The fluid domain consisted of 44,425 first-order flow-condition-based interpolation elements (45,276 nodes).[35] The fluid was modeled as air with a density of 1.2 kg/m^3, a viscosity of 1.8×10^{-5} Pa·s, and a bulk modulus of 141 kPa. The inlet pressure was 11.1 cmH_2O.

The solid domain consisted of 16,907 second-order elements (68,454 nodes) and allowed for large strain and large deformation. The Ogden model[32,36] was used with linear stress–strain curves between strain values of −0.5 and 1, and Young's modulus values based on the rheometry data are listed in Table 2. The Ogden model material constants are used in the strain energy density calculation:

$$W_D = \sum_{n=1}^{N} \left(\frac{\mu_n}{\alpha_n} [\lambda_1^{\alpha_n} + \lambda_2^{\alpha_n} + \lambda_3^{\alpha_n} - 3] \right),$$

where W_D is the deviatoric strain energy density, μ_n and α_n are the Ogden constants, and λ denotes stretch. In the current study, the Ogden constants were obtained for each layer by using a sixth-order fit (i.e., $N = 6$ in the earlier equation) to linear stress–strain curves with corresponding slopes based on the modulus values listed in Table 2, as shown in Supplementary Table S1. Bulk modulus values were obtained by using the corresponding Young's modulus values and a Poisson's ratio of 0.499. Rayleigh damping was applied to the model, with damping constants of $\alpha = 19.894$ and $\beta = 12.5323 \times 10^{-5}$. The initial glottal gap width was 2 mm.

Time integration was second order with a time step size of 25×10^{-6} s. The fluid and solid domains were directly coupled by using a sparse solver. Only one-half of the domain was simulated, assuming symmetry, to reduce the computational cost. Verification studies were performed to ensure that the obtained results were reasonable given the chosen mesh and time step sizes.

Results

Mechanical stability

Scaffolds that were cross-linked with PEGTA were stable under continuous mechanical stimulation (Table 3). However, the PEGDA scaffolds were visibly fragmented after continuous phonation.

Table 3. Biomaterial Optimization for the Scaffold Materials with 0.50% Hyaluronic Acid, Different Gelation Concentrations, and 0.50% Polyethylene Glycol Di-Acrylate or Polyethylene Glycol Tetra-Acrylate Cross-Linker

Gelatin concentration (%)	*Cross-linker*	*Mechanical stability*	*Biochemical stability (CCM with 10% FBS)*	*Biochemical stability (CCM with 5% FBS)*	*Cell adhesion*
0.25	PEGDA	×	×	×	✓
0.25	PEGTA	✓	×	×	✓
0.10	PEGTA	✓	×	✓	✓
0.05	PEGTA	✓	✓	✓	×
0.02	PEGTA	✓	✓	✓	×
0.00	PEGTA	✓	✓	✓	×

The symbols ✓ and × show that the scaffold has passed or failed the associated test, respectively.
PEGDA, polyethylene glycol di-acrylate.

Table 4. Viscoelastic Properties of the Constituents of the Vocal Fold Replicas and the Hyaluronic Acid–Gelatin Hydrogels (0.50% Hyaluronic Acid, 0.10% Gelatin, and 0.50% Polyethylene Glycol Di-Acrylate or Polyethylene Glycol Tetra-Acrylate)

Constituents	*Shear elastic modulus at 1.0 Hz (Pa)*	*Loss modulus at 1.0 Hz (Pa)*	*Shear elastic modulus at 10.0 Hz (Pa)*	*Loss modulus at 10.0 Hz (Pa)*
Dragon Skin	6874.9 ± 347.5	342.0 ± 0.1	10342.5 ± 2202.6	1472.5 ± 392.4
Ecoflex 0010	1872.9 ± 6.4	238.3 ± 6.7	3231.0 ± 55.2	992.4 ± 20.7
HA–Ge–PEGDA	99.2 ± 1.8	1.7 ± 0.4	110.8 ± 4.8	4.5 ± 1.2
HA–Ge–PEGTA	188.6 ± 1.4	2.9 ± 0.5	196.3 ± 6.9	7.6 ± 1.9

Mean and standard deviations are shown for three replicates.

Biochemical stability

The HA–Ge hydrogel that was immersed in water did not change in shape or size after 7 days (Supplementary Fig. S2A). Among the hydrogels that were immersed in CCM with 10% FBS, those with 0.25% or 0.10% Ge were mostly degraded after 7 days. However, those with 0.05%, 0.02%, and 0.00% Ge were stable for at least 21 days (Supplementary Fig. S2B). A low concentration of Ge was found to impede cell adhesion based on the bright-field images obtained by using a wide-field fluorescence microscope, Nikon eclipse TE2000-U. Cells were loosely attached to the surface of the hydrogels with 0.05%, 0.02%, or 0.00% Ge at 24 h after culture. As such, a 0.10% Ge concentration was found to be optimal. CCM with 5% FBS supports cell viability without adverse effects on the degradation rate of the HA-Ge scaffolds. At this FBS concentration, the CSM that was cross-linked with PEGDA or PEGTA (0.50% HA, 0.10% Ge, and 0.50% cross-linker) was biochemically stable over 21 days. These results are summarized in Table 3.

Rheometry

The viscoelastic properties of the silicone constituents of the replicas, and those of the HA–Ge hydrogels, for the frequencies of 1.0 and 10.0 Hz, are shown in Table 4. The shear elastic and loss moduli of the hydrogels that were cross-linked with PEGTA were greater than those of the PEGDA hydrogels. The viscoelastic properties of the silicone rubbers and those of the hydrogels slightly increased for the frequency of 10.0 Hz in comparison to the associated values for 1.0 Hz. The oscillatory stress–strain curve showed a linear elastic behavior for the HA–Ge hydrogels (0.50% HA, 0.10% Ge, and 0.50% PEGTA) over a wide range of strains (1–80%), as shown in Supplementary Figure S3.

Phonatory characteristics measurements

The average values and the standard deviations of the onset phonatory characteristics (the minimum lung pressures required to initiate vibration, including static and dynamic subglottal pressures, the associated dynamic supraglottal pressure, and the fundamental frequency) of the bioreactors are shown in Table 5. The phonatory characteristics of the bioreactors injected with the optimal HA–Ge hydrogel were obtained for static subglottal pressures greater than the associated onset pressure. The representative data are shown in Table 5. One typical measured dynamic subglottal pressure from one of the bioreactors is shown in the time and frequency domains in Figure 5. The dynamic subglottal pressure was periodic and resembled that associated with human VF self-oscillations.[37] The fundamental frequency of the bioreactor VF oscillations was around 100 Hz.

The static subglottal pressure for normal human phonation is reported to be around 13.7 cmH_2O.[37] For this static subglottal pressure, the peak-to-peak amplitude of the dynamic subglottal pressures was around 14.9 cmH_2O in our bioreactor, which is greater than the value of 9.6 cmH_2O obtained from a male subject for the normal phonation of the vowel /æ/.[37] However, the mentioned dynamic subglottal pressure can be achieved for a slightly lower static subglottal pressure in the bioreactor. The fundamental frequency of the bioreactor VF oscillations, that is, around 100 Hz, falls within the range of the fundamental frequency of male phonation.[37] The standard deviations of the measured values from different sets of phonation were within 10%. The measured radiated sound pressure level was 101 dB about 10 cm distance away from the folds in the incubator. The signal was noisier than that of the pressure transducer, owing to extraneous noise from the blower and reverberation inside the incubator enclosure. The fundamental frequency of the supraglottal pressure was the same as that of the pressure transducer, as expected.

Cell viability

The mean ± standard deviation of the viability rate was 95.2% ± 1.5% at the zero time point, 90.4% ± 5.2% in the control, and 91.3% ± 2.4% in the phonated samples at the

Table 5. Phonatory Characteristics of the Bioreactor

Static subglottal pressure (cmH_2O)	*Dynamic subglottal pressure (cmH_2O)*	*Dynamic supraglottal pressure (dB)*	*Fundamental frequency (Hz)*
11.1 ± 0.1	**2.1 ± 0.1**	**85.0 ± 2.0**	**93.8 ± 20.4**
12.4 ± 0.1	12.0 ± 0.1	101.0 ± 4.0	95.6 ± 18.5
13.6 ± 0.1	14.9 ± 0.1	106.0 ± 2.0	97.5 ± 19.1

The onset characteristics are shown in bold. The last two rows show the data achieved for two representative static subglottal pressures greater than the onset counterpart. Means and standard deviations are shown for three replicates.

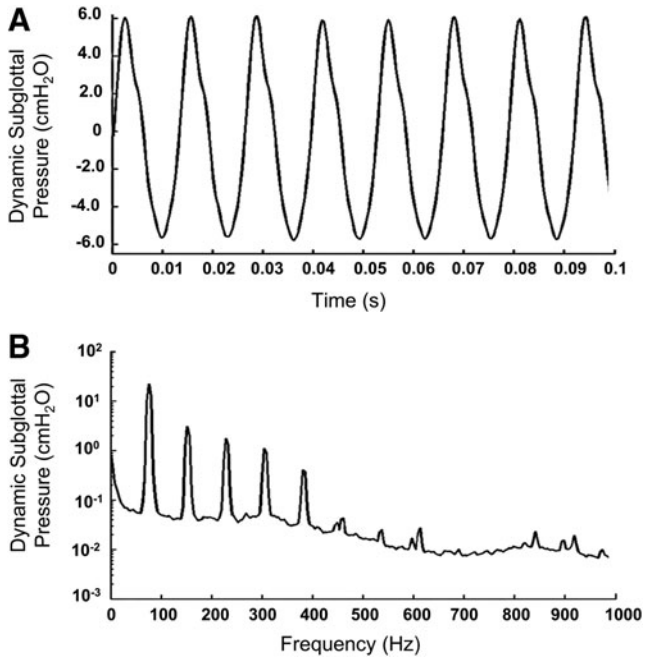

FIG. 5. One typical example of the dynamic subglottal pressure signature in the time **(A)** and frequency **(B)** domains.

end point of the study, that is, 7 days after the injection. The viability rate was 94.5% ± 4.1% in the samples that were cultured in the static condition.

ECM proteins synthesis

Figure 6A–C shows representative Col-I images of the zero time point, the control, and the phonated samples, respectively. Col-I and cell nuclei are shown in green and blue fluorescent, respectively. The 3D image of a phonated sample stained for Col-I is shown in Figure 6D. The cells were homogenously encapsulated in the CSM, and Col-I positive staining was detected at both the vicinity of the cell membrane and away from the cells inside the scaffold, 7 days after the injection. Representative Col-III images of the zero time point, the control, and the phonated samples are shown in Figure 7A–C, respectively. Positive Col-III staining was observed mostly in the vicinity of the cell membrane 7 days after the injection.

The Col-I level was greater in the phonated samples (0.0262 ± 0.0017) than in the controls (0.0066 ± 0.0005), as shown in Figure 8A. The Col-III level was greater in the phonated samples (0.0133 ± 0.0013) than in the controls (0.0059 ± 0.0020), as shown in Figure 8B.

Computational model

Figure 9 shows the simulated glottal width versus time waveforms. The model has reached a nearly steady-state oscillation pattern after about 0.14 s. The frequency was 82 Hz, which is close to that measured for the VF replicas (Table 5). Figure 10 shows the model at 12 different time points during one period of oscillation from about $t = 0.190 - 0.202$ s. The effective stress within the CSM is shown. Verification studies showed that the results were mesh and time step independent.

Discussion

Bioreactor concept

The large dimensions of the CSM limited the use of passive transport with sub-millimeter diffusion ranges. Mass

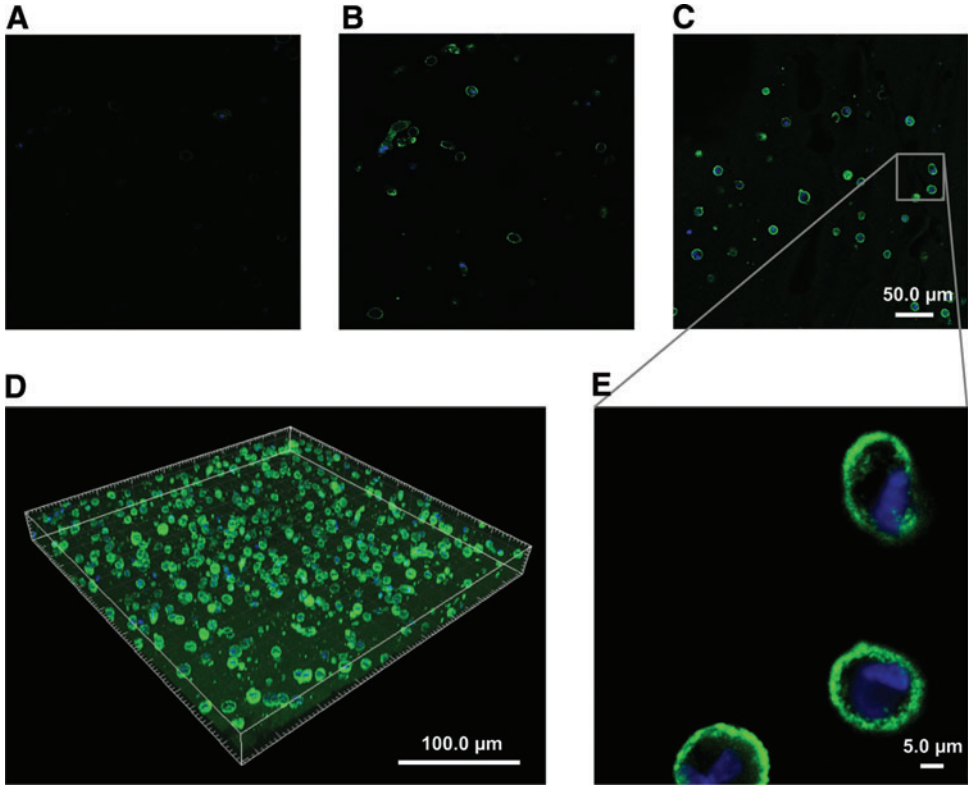

FIG. 6. Col-I synthesis inside the HA–Ge hydrogel at the **(A)** zero time point, **(B)** after 7 days in the control with CCM flow and without phonation, and **(C)** after 7 days of culture in the bioreactor with phonation. Col-I and cell nuclei are stained in *green* and *blue*, respectively. The images were captured with a 20× objective. **(A–C)** Scale bar is 50.0 μm. **(D)** A 3D-reconstructed image of Col-I and nuclei after 7 days of culture in the bioreactor. The cells were homogeneously encapsulated in the CSM, and Col-I positive staining was detected both in the vicinity of the cell membrane and throughout the CSM, 7 days after the injection. **(E)** Picture of the Col-I synthesis in the phonated sample with higher magnification (20×, zoom = 6). Col-I, collagen type I; Ge, gelatin; HA, hyaluronic acid. Color images available online at www.liebertpub.com/tec

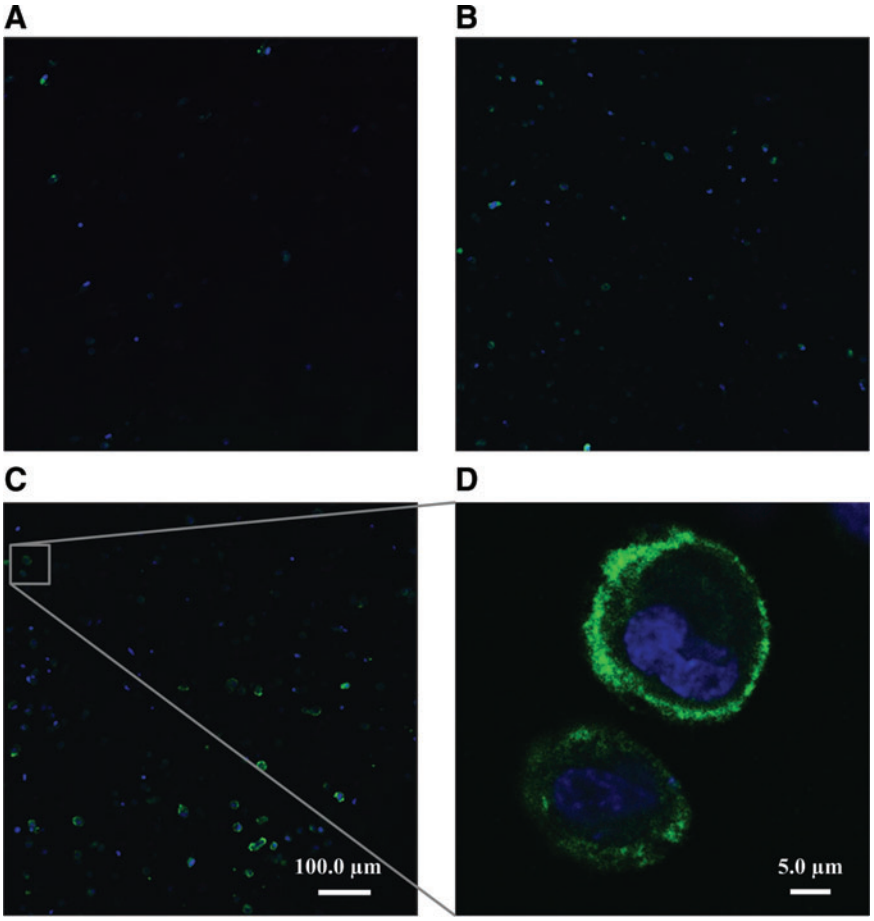

FIG. 7. Col-III synthesis inside the HA–Ge hydrogel at the **(A)** zero time point, **(B)** after 7 days in the control with CCM flow perfusion and without phonation, and **(C)** after 7 days of culture in the bioreactor with phonation. Col-III and cell nuclei are stained in *green* and *blue*, respectively. All the images were captured by using a 20× objective. **(A–C)** Scale bar is 50.0 μm. **(D)** Picture of the Col-III synthesis in the phonated sample with higher magnification (20×, zoom = 10). Col-III, collagen type III. Color images available online at www.liebertpub.com/tec

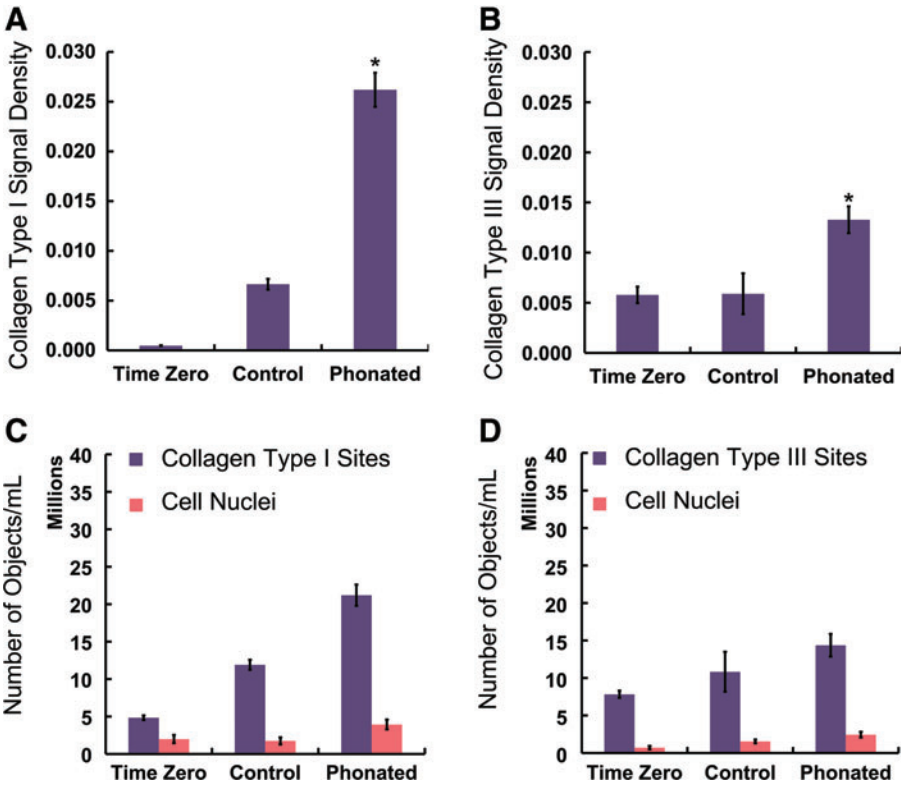

FIG. 8. **(A)** The Col-I signal densities at the zero time point (called ''Time Zero'' in this figure), for the controls with CCM flow perfusion and without phonation, and for the phonated samples with CCM flow perfusion and phonation. The signal densities are calculated as the ratio of volume of the detected protein to the volume of the image. **(B)** The Col-III signal densities. The Col-I and Col-III synthesis was greater in the phonated samples, and the differences were statistically significant ($p < 0.05$). There were no statistical differences in the Col-III densities between the controls and the zero time point samples ($p > 0.05$). * indicates a statistical significant difference. **(C, D)** Show the normalized number of objects expressing Col-I and Col-III, respectively, as well as the normalized number of cells to the volume of the image. The difference shows the normalized number of objects separated from the cells. The data are shown for three bioreactors. The error bars represent the standard deviations. Color images available online at www.liebertpub.com/tec

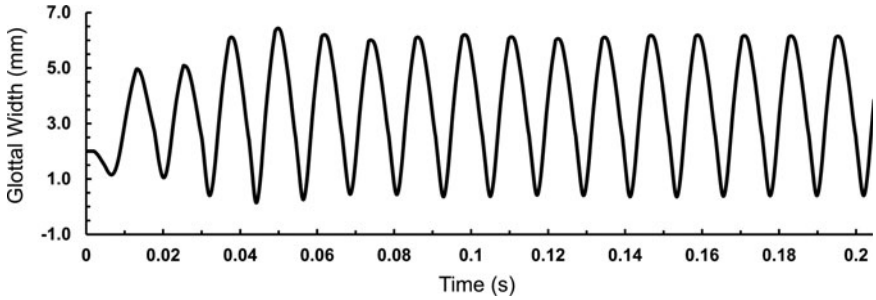

FIG. 9. Glottal gap width versus time from the computer simulation. The glottal gap is the gap between the vocal fold replicas.

transport was achieved throughout the confined perfusion of the nutrients. In our bioreactor, a flow rate of 0.01 mL/min was found to ensure a physiological pH balance (i.e., 7.4 ± 0.1) in the input and output flow, and to maintain cell viability during the test period. Such a flow rate has been previously shown to enhance the viability and proliferation of MC3T3-E1 osteoblast-like cells in a 3D culture with negligible effects on the genes expressed, compared with those of a 3D static culture.[38]

The present bioreactor design evolved through several generations of physical replicas of the human larynx built over the past 20 years to mimic phonation, particularly the fold collisions, *in vitro*.[34,39,40] The oscillation frequency, onset phonatory characteristics, and pressure-versus-flow characteristics of synthetic replicas without inner cavities were previously shown to be in the range of those of human phonation.[22,41] The concept of physical replicas was modified by the introduction of an inner cavity to host the CSM. From our previous study, two sets of replicas were examined: two layer (a layer of Ecoflex and a layer of the CSM) and three layer (the two-layer replica plus a thin layer of Dragon Skin).[25]

The onset phonatory characteristics were investigated for each bioreactor for different scaffold materials.[25] The onset static subglottal pressure decreased for the three-layer bioreactors compared with the associated two-layer counterparts. In other words, the three-layer bioreactor required smaller subglottal pressure to start oscillating, indicating that the addition of the Dragon Skin layer facilitates VF self-sustained oscillations at lower pressures. The onset static subglottal pressure decreased with an increase in the shear elastic modulus of the hydrogel. The viscoelastic properties of the injected material were shown to affect the onset static subglottal pressure, and the associated dynamic subglottal and supraglottal pressures.[25] The present study was performed by using the three-layer replica.

The current bioreactor design allows the adjustment of the subglottal pressure by using a pressure-regulating valve, which controls the speed of the centrifugal blower. The pressure adjustment, in turn, allows the control of the phonation frequency and the airflow rate. The radiated sound pressure and oscillation amplitude of the VF replicas also change with the subglottal pressure. In addition, the bioreactor design allows systematic variation of the pre-phonatory glottal width (PPGW) and pre-phonatory VF stretch (PPS). The variation of the PPGW provides alteration of the relative prevalence of impact-related stresses

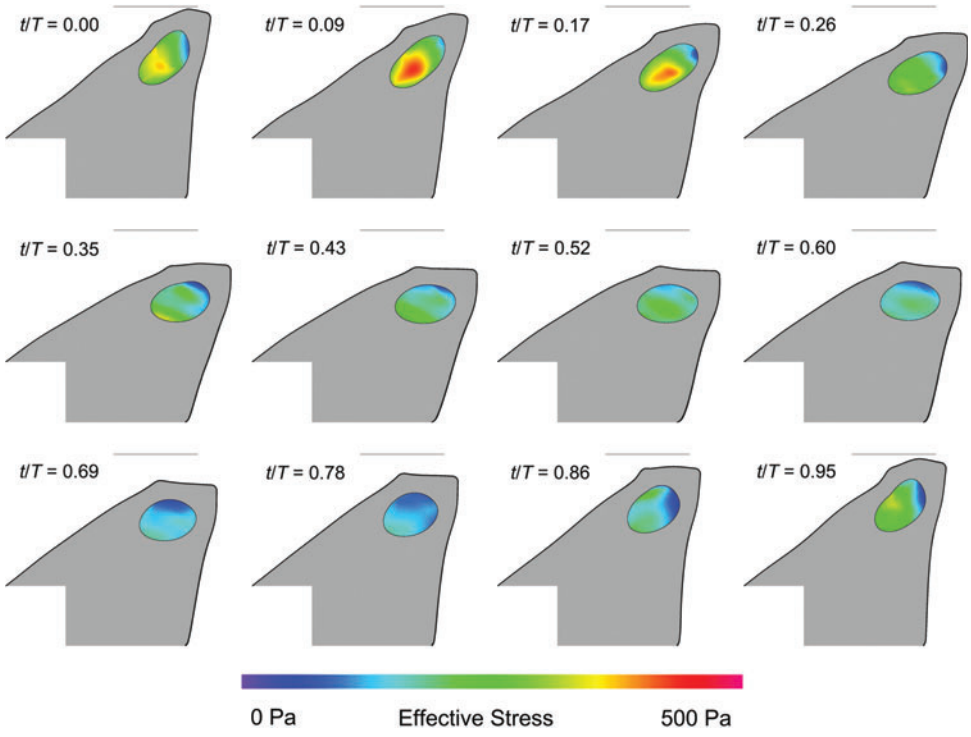

FIG. 10. One period of oscillation of replica simulation showing model deformation, cavity (CSM) deformation, and cavity effective stress. The *light gray line* in each frame denotes the approximate location of the symmetry line. Time stamps denote fraction of one period. Color images available online at www.liebertpub.com/tec

over elastic or aerodynamic stresses within the scaffold.[42] Excessive impact stresses are postulated to induce cell death[43] or cell migration away from the VF surface. The PPS causes a longitudinal strain, which may influence the orientation of collagen fibers in the engineered ECM. The 10% PPS used in the present study was established based on data obtained by using high-speed digital images of three human subjects' VFs.

Additional requirements were considered for the design of the new bioreactor. The biocompatibility of the materials used to fabricate the replicas was investigated. The Ecoflex silicone rubber used in the current bioreactor was found not to elicit any adverse reaction in the VF fibroblasts cultured inside the HA–Ge hydrogels based on our viability studies. The Ecoflex silicone rubber can also withstand numerous cycles of high temperature and pressure without losing its primary shape and dimensions. Therefore, it is possible to autoclave the bioreactor body to sterilize the inner cavity of the replicas. The mechanical longevity test also showed only minor variations (<15%) in frequency, thereby demonstrating the replicas' potential for extended mechanical longevity.

Biomaterial selection and optimization

HA and its derivatives have been widely investigated as hydrogels for VF tissue engineering due to their excellent biocompatibility, biodegradability, and gel-forming properties.[2,3,44] HA is a natural, negatively charged glycosaminoglycan that is widely distributed within the LP. HA plays a significant role in important biological processes such as tissue hydration, nutrient diffusion, proteoglycan organization, and cell differentiation, as well as in the tissue viscoelastic properties.[45] It is naturally degraded by hyaluronidase, allowing the degradation to be controlled by the cells that are encapsulated inside the scaffold.[46] Gelatin is formed by breaking the natural triple-helix structure of collagen into single-strand molecules[47] and is less immunogenic than intact collagen. Gelatin promotes cell adhesion, migration, differentiation, and proliferation.[45] Gelatin is naturally degraded by metalloproteases, specifically collagenase, and serine proteases that allow for degradation to be locally controlled by the cells.

The introduction of Ge into HA hydrogels was shown to significantly improve the adhesion and migration of fibroblasts.[2,46] Native HA in its uncross-linked form provides a short half-life *in vivo*. The degradation rate of HA-based hydrogels by covalent cross-linking of the modified HA using PEGDA was found to yield lower degradation rates.[3] The HA–Ge hydrogel used in the present study was optimized for its biochemical and mechanical stability (Table 3). Although the biochemical stability of the scaffold is affected by the cross-linker type and concentration, the presence of Ge in the structure makes it prone to enzymatic degradation. Decreasing Ge concentration improved the biochemical stability. However, Ge concentrations below 0.10% decreased cell adhesion. A concentration of 0.10% Ge was selected. The concentration of FBS in CCM also affects the scaffold degradation. With 5% FBS, CCM was observed to support cell viability without adverse degradation of the scaffold. Further, the HA–Ge scaffolds that cross-linked with PEGDA and PEGTA at this concentration were biochemically stable over a 21-day period.

A stiffer scaffold was obtained by using PEGTA in comparison to PEGDA, as shown in Table 4. The shear elastic moduli of both the PEGDA and PEGTA hydrogels were within the range of that of the human VF LP.[48] Polymeric materials may fail under cyclic loading. The scaffolds made of HA, Ge, and PEGTA were mechanically stable under continuous phonation-induced stimulation. However, HA–Ge–PEGDA scaffolds were fragmented after continuous phonation. PEGTA has four arms for linking HA and Ge molecules, which yields an increase in strength and the capacity for absorbing energy during cyclic loading. Therefore, a 0.50% HA, 0.10% Ge, and 0.50% PEGTA mixture was deemed optimal for our bioreactor studies.

Bioreactor verification

The phono-mimetic bioreactor was assessed in terms of cell viability and cellular function of ECM synthesis. The viability rates were >90.0% for the phonated, the controls, and the zero time point samples. The total number of cells per mL, that is, cell density, was increased in the phonated samples compared with those of the controls and the zero time point samples. Stable well-differentiated cells inside the bioreactor will facilitate the long-term study of the cellular behavior under specific biomechanical stimulation.

Positive Col-I and Col-III staining was detected in the vicinity of the cell membrane and inside the scaffold in the phonated samples, as shown in Figures 6C–E and 7C, D, respectively. The Col-I synthesis was greater in the phonated sample compared with the controls and the zero time point samples (Fig. 8A). These results showed that the biomechanical stimulation in our bioreactor promotes Col-I synthesis. The number of Col-I objects per mL of the CSM was greater than the total number of cells per mL in all samples (Fig. 8C). The difference shows the number of Col-I objects away from the cells after synthesis. Similar observations were made for Col-III. Greater Col-III synthesis was observed in the phonated samples compared with the controls and the zero time point samples (Fig. 8B). The Col-I signal density (0.0262 ± 0.0017) was greater than that of Col-III (0.0133 ± 0.0013) in the phonated samples. The number of Col-III objects separated from the cells was greater than the number of cells in all the samples (Fig. 8D).

Our results suggest that HVFFs were able to maintain their function of collagen synthesis in the present bioreactor environment. The phono-mimetic stimulation enhanced Col-I and Col-III synthesis. These results are generally consistent with those from previous VF bioreactors, which reported an increase in cell density and collagen synthesis in the stimulated samples compared with the associated unstimulated controls.[9,10] However, it is difficult to make any conclusive quantitative comparisons with results from previous studies because of many inconsistencies in cell types, scaffold materials, and methods, as summarized in Table 1.

Our bioreactor is easy to assemble, relatively reproducible, inexpensive, and disposable. The design offers a completely closed culture environment that minimizes the possibility of contamination within the CSM, and it facilitates long-term cellular stimulation in a controlled environment.

Computational models are needed to quantify the mechanical forces acting on the cells and the deformations of the CSM in the VF replicas of our bioreactor for further mechanobiology investigations, as direct measurements are local and difficult to perform.[22,41,49] The developed computational model (Fig. 4) demonstrated a potential mechanism

for estimating the stress and strain fields over time within the CSM (Fig. 10). Computational simulation in conjunction with experimental data will reveal how complex mechanical forces acting on VF cells determine the viability, mobility, and organization of engineered VF ECM components.

Future directions

Detailed comparisons with an electro-acoustically driven bioreactor are planned to further characterize the impact of the phono-mimetic biomechanical stimulation.[15] The scaffold shape and dimensions of our VF replicas will be refined to better mimic the three-layer morphology of the LP and the volume occupied by the muscle. Automated digital controls for static subglottal pressure, airflow rate, and the VF longitudinal prestretch will be implemented to allow the operation of several bioreactors simultaneously. One bioreactor will then be used as a control for the longitudinal prestretch, that is, with phonatory stimulation and without longitudinal prestretch. This will facilitate further studies, for example of the influence of the longitudinal prestretch on the cell behavior.

The HVFFs used in the present study were from an immortalized cell line, which has been previously shown to exhibit genotype and phenotype characteristics similar to those in primary cells natively.[50] Primary VF fibroblasts are typically very difficult to obtain in adequate numbers. Immortalized HVFFs are, however, a reproducible characterized source of VF fibroblasts that provide an unlimited source of cells.[50] As part of our future directions, we will culture primary HVFFs inside our bioreactor.

Conclusions

A novel VF bioreactor system was designed, built, and validated. Key bioreactor phonatory characteristics were found to be within the range of male human phonation. The phono-mimetic biomechanical stimulation was found to cause scaffold fragmentation in some cases, prompting the need for more robust scaffold materials. The confined flow perfusion design caused biochemical degradation of the scaffold by some ingredients of the CCM, mainly the FBS. Our results demonstrated that the bioreactor supports cell viability and enhances collagen synthesis.

Such a bioreactor helps future investigations of the effects of different phonatory characteristics on the behavior of VF cells in terms of viability and collagen synthesis, *in vitro*. The data will be used to design behavioral treatments for patients with voice disorders, particularly post-surgical voice regimes for those who have lost a portion of their LP. This bioreactor also facilitates VF tissue engineering investigations in a systematically controlled environment. For instance, it can be used for the development and optimization of injectable biomaterials in terms of mechanical and biochemical stability. The use of the proposed bioreactor also decreases the number of animals that are needed to investigate the long-term outcome of VF-specific biomaterials.

Acknowledgments

This work was supported by grants R01-DC005788 (L.M.) and R03DC012112 (N.Y.K.L.-J.) from the National Institutes of Health (NIDCD). The authors would like to thank Professor Susan Thibeault (Department of Surgery, University of Wisconsin) for providing the HVFFs, Dr. Eric Boucher (Department of Anatomy and Cell Biology, McGill University) for many fruitful discussions, Chanwoo Yang and Scott Sang Park (Department of Mechanical Engineering, McGill University) for their help in the fabrication of the replicas, and Merlyn Christopher (Department of Mechanical Engineering, McGill University) for her help with the figures. The work of Preston Murray (Department of Mechanical Engineering, Brigham Young University) in designing early replica models and of Shelby Dushku and Kim Stevens (Department of Mechanical Engineering, Brigham Young University) in performing mechanical longevity studies is also gratefully acknowledged. The authors also thank the Advanced Bio Imaging Facility (Life Sciences Complex, McGill University) for allowing them to use their facility. This work was performed in the following laboratories: Biomechanics Research Laboratory, Department of Mechanical Engineering, McGill University (817 Sherbrooke Street West, Montreal, QC H3A 0C3, Canada); Prof. Vali's Laboratory, Department of Anatomy and Cell Biology, McGill University (Room 1/45-47, 3640 University Street, Montreal, QC H3A 2B2, Canada); and McGill University Life Sciences Complex Advanced BioImaging Facility (ABIF) (3649 Promenade Sir William Osler, Bellini Building, Montreal, QC H3G 0B1, Canada).

Disclosure Statement

No competing financial interests exist.

References

1. Li, N., Heris, H., and Mongeau, H. Current understanding and future directions for vocal fold mechanobiology. J Cytol Mol Biol **1,** 1, 2013.
2. Duflo, S., Thibeault, S.L., Li, W., Shu, X.Z., and Prestwich, G.D. Vocal fold tissue repair in vivo using a synthetic extracellular matrix. Tissue Eng **12,** 2171, 2006.
3. Heris, H.K., Rahmat, M., and Mongeau, L. Characterization of a hierarchical network of hyaluronic acid/gelatin composite for use as a smart injectable biomaterial. Macromol Biosci **12,** 202, 2012.
4. Tong, Z., and Jia, X. Biomaterial-based strategies for the engineering of mechanically active soft tissues. MRS communications **2,** 31, 2012.
5. Tong, Z., Zerdoum, A.B., Duncan, R.L., and Jia, X. Dynamic vibration cooperates with connective tissue growth factor to modulate stem cell behaviors. Tissue Eng Part A **20,** 1922, 2014.
6. Ishii, K., Yamashita, K., Akita, M., and Hirose, H. Age-related development of the arrangement of connective tissue fibers in the lamina propria of the human vocal fold. Ann Otol Rhinol Laryngol **109,** 1055, 2000.
7. Hartnick, C.J., Rehbar, R., and Prasad, V. Development and maturation of the pediatric human vocal fold lamina propria. Laryngoscope **115,** 4, 2005.
8. Hirano, M., Kurita, S., and Nakashima, T. Growth, development and aging of human vocal folds. In: Bless, D.M., and Abbs, J.H., eds. Vocal Fold Physiology: Contemporary Research and Clinical Issues. San Diego, CA: College-Hill Press, 1983, p. 22.
9. Titze, I.R., Hitchcock, R.W., Broadhead, K., Webb, K., Li, W., Gray, S.D., and Tresco, P.A. Design and validation of a

bioreactor for engineering vocal fold tissues under combined tensile and vibrational stresses. J Biomech **37,** 1521, 2004.
10. Wolchok, J.C., Brokopp, C., Underwood, C.J., and Tresco, P.A. The effect of bioreactor induced vibrational stimulation on extracellular matrix production from human derived fibroblasts. Biomaterials **30,** 327, 2009.
11. Kutty, J.K., and Webb, K. Vibration stimulates vocal mucosa-like matrix expression by hydrogel-encapsulated fibroblasts. J Tissue Eng Regen Med **4,** 62, 2010.
12. Branski, R.C., Perera, P., Verdolini, K., Rosen, C.A., Hebda, P.A., and Agarwal, S. Dynamic biomechanical strain inhibits IL-1β-induced inflammation in vocal fold fibroblasts. J Voice **21,** 651, 2007.
13. Gaston, J., Rios, B.Q., Bartlett, R., Berchtold, C., and Thibeault, S.L. The response of vocal fold fibroblasts and mesenchymal stromal cells to vibration. PloS One **7,** e30965, 2012.
14. Farran, A.J., Teller, S.S., Jia, F., Clifton, R.J., Duncan, R.L., and Jia, X. Design and characterization of a dynamic vibrational culture system. J Tissue Eng Regen Med **7,** 213, 2013.
15. Tong, Z., Duncan, R.L., and Jia, X. Modulating the behaviors of mesenchymal stem cells via the combination of high-frequency vibratory stimulations and fibrous scaffolds. Tissue Eng Part A **19,** 1862, 2013.
16. Martin, I., Wendt, D., and Heberer, M. The role of bioreactors in tissue engineering. Trends Biotechnol **22,** 80, 2004.
17. Bancroft, G.N., Sikavitsas, V.I., and Mikos, A.G. Technical note: design of a flow perfusion bioreactor system for bone tissue-engineering applications. Tissue Eng **9,** 549, 2003.
18. Gardel, L.S., Serra, L.A., Reis, R.L., and Gomes, M.E. Use of perfusion bioreactors and large animal models for long bone tissue engineering. Tissue Eng Part B Rev **20,** 126, 2013.
19. Goldstein, A.S., Juarez, T.M., Helmke, C.D., Gustin, M.C., and Mikos, A.G. Effect of convection on osteoblastic cell growth and function in biodegradable polymer foam scaffolds. Biomaterials **22,** 1279, 2001.
20. Bilodeau, K., Couet, F., Boccafoschi, F., and Mantovani, D. Design of a perfusion bioreactor specific to the regeneration of vascular tissues under mechanical stresses. Artif Organs **29,** 906, 2005.
21. Watanabe, S., Inagaki, S., Kinouchi, I., Takai, H., Masuda, Y., and Mizuno, S. Hydrostatic pressure/perfusion culture system designed and validated for engineering tissue. J Biosci Bioeng **100,** 105, 2005.
22. Murray, P.R., and Thomson, S.L. Vibratory responses of synthetic, self-oscillating vocal fold models. J Acoust Soc Am **132,** 3428, 2012.
23. Scherer, R.C., Shinwari, D., De Witt, K.J., Zhang, C., Kucinschi, B.R., and Afjeh, A.A. Intraglottal pressure profiles for a symmetric and oblique glottis with a divergence angle of 10 degrees. J Acoust Soc Am **109,** 1616, 2001.
24. Chhetri, D.K., Zhang, Z., and Neubauer, J. Measurement of Young's modulus of vocal folds by indentation. J Voice **25,** 1, 2011.
25. Latifi, N., Heris, H.K., Kazemirad, S., and Mongeau, L. Development of a self-oscillating mechanical model to investigate the biological response of human vocal fold fibroblasts to phono-mimetic stimulation. In: ASME 2014 International Mechanical Engineering Congress and Exposition. Montreal: American Society of Mechanical Engineers, 2014, p. V003T03A002.
26. Murray, P.R., and Thomson, S.L. Synthetic, multi-layer, self-oscillating vocal fold model fabrication. J Vis Exp e3498, 2011.
27. Park, I.S., Kim, S.H., Heo, D.N., Jung, Y., Kwon, I.K., Rhie, J.-W., and Kim, S.-H. Synergistic effect of biochemical factors and strain on the smooth muscle cell differentiation of adipose-derived stem cells on an elastic nanofibrous scaffold. J Biomater Sci Polym Ed **23,** 1579, 2012.
28. Youngstrom, D.W., Rajpar, I., Kaplan, D.L., and Barrett, J.G. A bioreactor system for in vitro tendon differentiation and tendon tissue engineering. J Orthop Res **33,** 911, 2015.
29. Ridler, T., and Calvard, S. Picture thresholding using an iterative selection method. IEEE Trans Syst Man Cybern **8,** 630, 1978.
30. Lee, J.-S., Wee, T.-L.E., and Brown, C.M. Calibration of wide-field deconvolution microscopy for quantitative fluorescence imaging. J Biomol Tech **25,** 31, 2014.
31. Daily, D.J., and Thomson, S.L. Acoustically-coupled flow-induced vibration of a computational vocal fold model. Comput Struct **116,** 50, 2013.
32. Smith, S.L., and Thomson, S.L. Influence of subglottic stenosis on the flow-induced vibration of a computational vocal fold model. J Fluids Struct **38,** 77, 2013.
33. Smith, S.L., and Thomson, S.L. Effect of inferior surface angle on the self-oscillation of a computational vocal fold model. J Acoust Soc Am **131,** 4062, 2012.
34. Thomson, S.L., Mongeau, L., and Frankel, S.H. Aerodynamic transfer of energy to the vocal folds. J Acoust Soc Am **118,** 1689, 2005.
35. Bathe, K.-J., and Zhang, H. A flow-condition-based interpolation finite element procedure for incompressible fluid flows. Comput Struct **80,** 1267, 2002.
36. Zhang, K., Siegmund, T., and Chan, R.W. A constitutive model of the human vocal fold cover for fundamental frequency regulation. J Acoust Soc Am **119,** 1050, 2006.
37. Sundberg, J., Scherer, R., Hess, M., Müller, F., and Granqvist, S. Subglottal pressure oscillations accompanying phonation. J Voice **27,** 411, 2013.
38. Cartmell, S.H., Porter, B.D., García, A.J., and Guldberg, R.E. Effects of medium perfusion rate on cell-seeded three-dimensional bone constructs in vitro. Tissue Eng **9,** 1197, 2003.
39. Mongeau, L., Franchek, N., Coker, C.H., and Kubli, R.A. Characteristics of a pulsating jet through a small modulated orifice, with application to voice production. J Acoust Soc Am **102,** 1121, 1997.
40. Chen, L.-J., and Mongeau, L. Verification of two minimally invasive methods for the estimation of the contact pressure in human vocal folds during phonation. J Acoust Soc Am **130,** 1618, 2011.
41. Pickup, B.A., and Thomson, S.L. Flow-induced vibratory response of idealized versus magnetic resonance imaging-based synthetic vocal fold models. J Acoust Soc Am **128,** EL124, 2010.
42. Titze, I.R., Schmidt, S.S., and Titze, M.R. Phonation threshold pressure in a physical model of the vocal fold mucosa. J Acoust Soc Am **97,** 3080, 1995.
43. Torzilli, P., Borrelli, J., Helfet, D., and Grigiene, R. Effect of impact load on articular cartilage: cell metabolism and

viability, and matrix water content. J Biomech Eng **121,** 433, 1999.
44. Tan, H., and Marra, K.G. Injectable, biodegradable hydrogels for tissue engineering applications. Materials **3,** 1746, 2010.
45. Chan, R.W., Gray, S.D., and Titze, I.R. The importance of hyaluronic acid in vocal fold biomechanics. Otolaryngol Head Neck Surg **124,** 607, 2001.
46. Shu, X.Z., Liu, Y., Palumbo, F., and Prestwich, G.D. Disulfide-crosslinked hyaluronan-gelatin hydrogel films: a covalent mimic of the extracellular matrix for in vitro cell growth. Biomaterials **24,** 3825, 2003.
47. Nicodemus, G.D., and Bryant, S.J. Cell encapsulation in biodegradable hydrogels for tissue engineering applications. Tissue Eng Part B Rev **14,** 149, 2008.
48. Chan, R.W., and Titze, I.R. Viscoelastic shear properties of human vocal fold mucosa: measurement methodology and empirical results. J Acoust Soc Am **106,** 2008, 1999.
49. Decker, G.Z., and Thomson, S.L. Computational simulations of vocal fold vibration: Bernoulli versus Navier–Stokes. J Voice **21,** 273, 2007.
50. Chen, X., and Thibeault, S.L. Novel isolation and biochemical characterization of immortalized fibroblasts for tissue engineering vocal fold lamina propria. Tissue Eng Part C Methods **15,** 201, 2008.

Address correspondence to:
Neda Latifi, MSc
Department of Mechanical Engineering
McGill University
817 Sherbrooke Street West
Montreal H3A 0C3
Quebec
Canada

E-mail: neda.latifialavijeh@mail.mcgill.ca

Received: February 12, 2016
Accepted: July 11, 2016
Online Publication Date: August 15, 2016